applied sciences

MDPI

Article

System Development for Diffusion Bonding of Multiple Unit Tubes to Produce Long Tubular Tungsten Heavy Alloys

Zu Seong Park [1], Young Yun Woo [2], Sang Wook Han [2], Il Yeong Oh [2], Tae Woo Hwang [2], Yangjin Kim [2] and Young Hoon Moon [2,*]

1 R&D Center, Poongsan, 2606-10 Hokook-ro, Angang, Gyeongju, Gyeongsangbuk-do 38026, Korea; zu-seong.park@poongsan.co.kr

2 School of Mechanical Engineering, Pusan National University, Geumjeong-gu, Busan 46241, Korea; yywoo@pusan.ac.kr (Y.Y.W.); swhan@pusan.ac.kr (S.W.H.); iyoh@pusan.ac.kr (I.Y.O.); twhwang@pusan.ac.kr (T.W.H.); yangjin@pusan.ac.kr (Y.K.)

* Correspondence: yhmoon@pusan.ac.kr; Tel.: +82-51-510-2472

Received: 5 March 2020; Accepted: 22 April 2020; Published: 24 April 2020

Abstract: A diffusion bonding system to fabricate long tubular parts by joining of two- or more-unit tubes made of tungsten heavy alloys (THAs) is proposed and characterized in this study. The difficulty of powder processing of THA originates from the weak strength of the green compact and the high weight of the THA powders. The long tubular green compact is difficult to handle due to its weak structural integrity. Furthermore, gravity-induced slumping during liquid phase sintering induces dimensional distortion and degrades the mechanical performances. As a clue for solving these problems, the unit tubes are fabricated. However, the mass of green compacts for unit tubes is not sufficiently great as to cause problematic slumping; tubular unit tubes can be obtained without significant difficulty. Fabricated unit tubes are stacked in a furnace chamber and diffusion-bonded to produce a long tubular part having bond strength substantially equal to that of a monolithic tube. The proposed diffusion bonding system was well characterized and successfully applied to the industrial production line. The feasibility was also confirmed by investigating the bond quality, which can be assessed by metallographic microstructure and mechanical property.

Keywords: diffusion bonding; tungsten heavy alloy; tube; liquid phase sintering; sinter bonding

1. Introduction

Tungsten heavy alloys (THAs) are a typical class of multi-phase composites consisting of tungsten powders embedded in a ductile matrix phase with lower melting point binder metals such as Ni, Fe, Cu, and Co. As the melting point of tungsten is excessively high, binder metals have been mixed to form a liquid phase when heated to a moderate temperature. The melted binder metals induce wetting of the tungsten grains, leading to the attainment of full density through the tungsten grain densification and rearrangement [1,2]. As tungsten is the practical element for a wide range of uses in density driven applications, THAs have been widely used in making counterbalance for vibration dampening, parts for military defense, such as missile weapons and fire arms, and in many applications that require long tubular or hollow shapes.

In general, conventional plastic forming processes, such as roll forming [3–6] and seamless tube manufacturing [7] methods, have been usually used to produce tubular parts. For relatively complex shaped products, hydroforming [8–11] and electromagnetic forming [12,13] have been used.

As tungsten is tough and difficult-to-form material, the application of the conventional plastic forming method to the fabrication of long tubular parts is hard to achieve. Furthermore, THAs have

low machinability because it is abrasive and produces short chips [14]. Therefore, although a variety of possible fabrication technologies exist for specific applications, almost all THA manufacture utilizes the powder metallurgy approaches.

The processing sequence of THAs includes the mechanical blending of the elemental powders and high- pressure powder compaction by cold pressing, followed by liquid phase sintering to obtain dense products [15,16]. The size of a green compact that can be produced using conventional powder metallurgy approaches can be limited by the relatively low green compact strength and the heavy weight of THA powders. As the green compact is easily broken, the shape of the green compact significantly influences its structural rigidity. Especially, long tubular compacts are hard to press in shaped tooling and challenging to handle. Another difficulty in producing a large THA compact through liquid phase sintering is gravity-induced slumping [17]. Even with the structural support of the compact, slumping is hard to prevent during liquid phase sintering. Accordingly, dimensional changes due to slumping need to be taken into account by considering the dimensional change of the compact after liquid phase sintering [18].

A method for fabricating long tubular parts by inductively bonding multiple unit tubes has been developed and industrially implemented [19]. To reduce the handling weight of green compacts, the unit tubes of small sintered compacts have been used for fabricating long products. The mass of unit tubes was not sufficiently high as to cause problematic slumping, long tubular products have been successfully obtained. However, as an inductive bonding typically present narrow stability windows [20–22], it demands tremendous efforts to control the processing parameters, such as temperature, vacuum level, pressing weight, and alignment positioning of the unit tubes to achieve high quality bonding.

Therefore, a useful diffusion bonding system has been proposed in this study to overcome the difficulties of the inductive bonding method. Unlike the local inductive bonding method, which requires multi-control of respective joints between unit tubes, the proposed diffusion bonding system heats entire unit tubes for easy and unified control. Multiple unit tubes are stacked in a specially designed heating chamber and diffusion bonded to produce a monolithic tube. In the optimization of the diffusion bonding process, the effect of processing factors, the tube positioning, temperature, and environment gas atmosphere on the bonding quality has been investigated. The feasibility of developed system has been confirmed by metallographic analysis of microstructures and mechanical testing.

2. Materials and Methods

2.1. Materials and Fabrication of Unit Tubes

The investigated THAs were fabricated from high pure elemental powders of 93.10 wt% W, 4.83 wt% Ni, and 2.07 wt% Fe. The raw powders were mechanically mixed to form a homogeneous blend. The blended tungsten alloy powders were ball-milled for 5 h in a jar filled with 1.0–1.5-inch balls in an argon environment to break up the agglomerates, provide intimate mixing, and uniformly disperse the elemental powders. For the homogeneous distribution, the blended powders were crushed again using a Fitz mill. Then, the powders were subjected to cold isostatic pressing (CIP) in order to obtain denser green compacts [23–26]. The assembly was pressurized hydrostatically in a chamber at 195 MPa for 20 s.

In this study, unit tubes have been fabricated by diffusion bonding of semicircular tubes shown in Figure 1a. Semicircular tubes were produced by liquid phase sintering of THA green compacts having semicircular shapes [27]. The sintered semicircular tubes were subsequently joined by solid state diffusion bonding at 1427 °C for 3 h, as shown in Figure 1b [28]. The outer diameter, wall thickness, and length of the unit tube are 205.0 mm, 20.0 mm, and 208 mm, respectively. Then, diffusion bonded tubes were machined to unit tubes having target shapes, as shown in Figure 1c. The process sequence for fabricating the unit tube is summarized in Figure 2.

(a) **(b)** **(c)**

Figure 1. Unit tube manufacturing: (**a**) sintered and machined semicircular tubes; (**b**) diffusion bonded tube; (**c**) final machined tube.

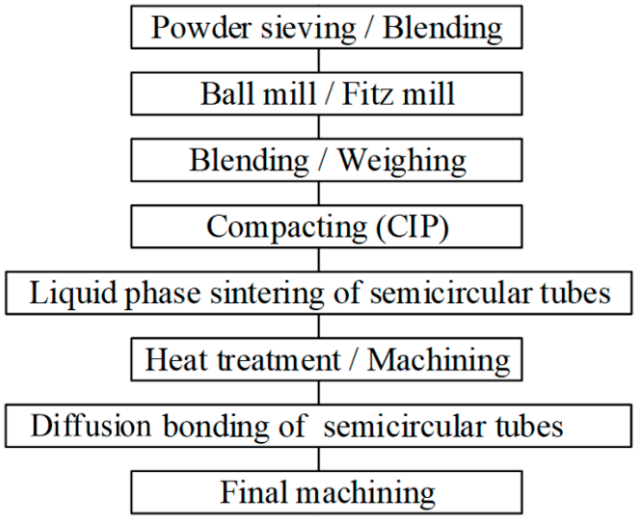

Figure 2. Process sequence for fabricating the unit tube.

2.2. System Design to Fabricate Long Tubular Products

In the fabrication of long tubular parts, a vertical type diffusion bonding system has been specially designed to conduct the following functions. Accurate measurement and control of temperature in high temperature processes are crucial and must be prioritized to maintain system performances [29–33]. Figure 3 schematically shows the diffusion bonding system developed in this study. The unit tubes are vertically positioned in a chamber of the diffusion bonding system. The unit tubes are stacked on a non-reactive firebrick cart to prevent possible contaminations, and then inserted into the chamber. The stacked unit tubes are diffusion bonded in the heating zone under a controlled gas atmosphere. As the junctures of the stacked unit tubes are heated to a solid-state sintering temperature, the alignment control of the stacked unit tubes to limit distortion and slumping is critical to obtain acceptable long tubular products. After the diffusion bonding process, the bonded products are cooled in the cooling zone under a controlled gas atmosphere.

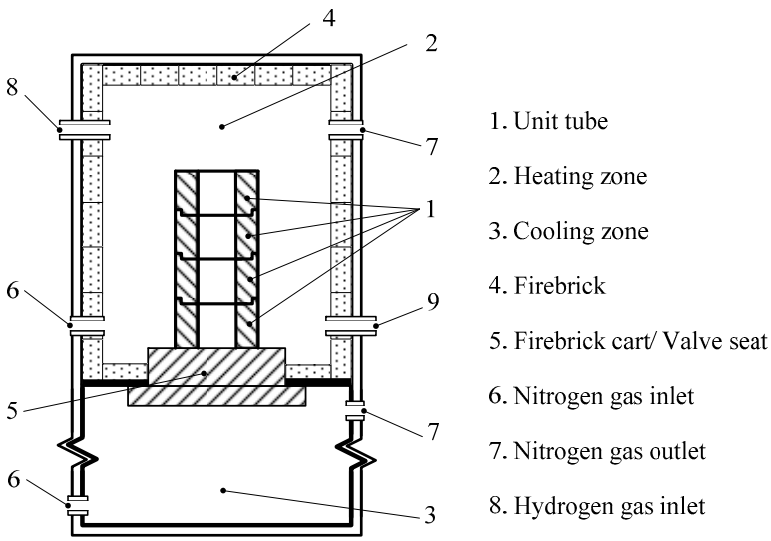

Figure 3. Schematic drawing of the diffusion bonding system.

Figure 4 provides schematic drawings of the vertical diffusion bonding system. Figure 4a shows stacked tubes before diffusion bonding. For diffusion bonding, stacked tubes are first loaded in the cooling zone, and then, the loading gate is closed. To evacuate air in the heating and cooling zones, nitrogen purging is performed to achieve a nitrogen atmosphere. Then, the stacked tubes are elevated and positioned at the heating zone and heated under controlled atmosphere for diffusion bonding, as shown in Figure 4b. The diffusion-bonded product is moved to the cooling zone and cooled by nitrogen circulation, as shown in Figure 4c. The product in the cooling zone is still at a high temperature, and thus, to prevent oxidation and surface deterioration, cooling by nitrogen circulation is continued until the temperature of the product reaches 150 °C. The product is then extracted from the system and air-cooled.

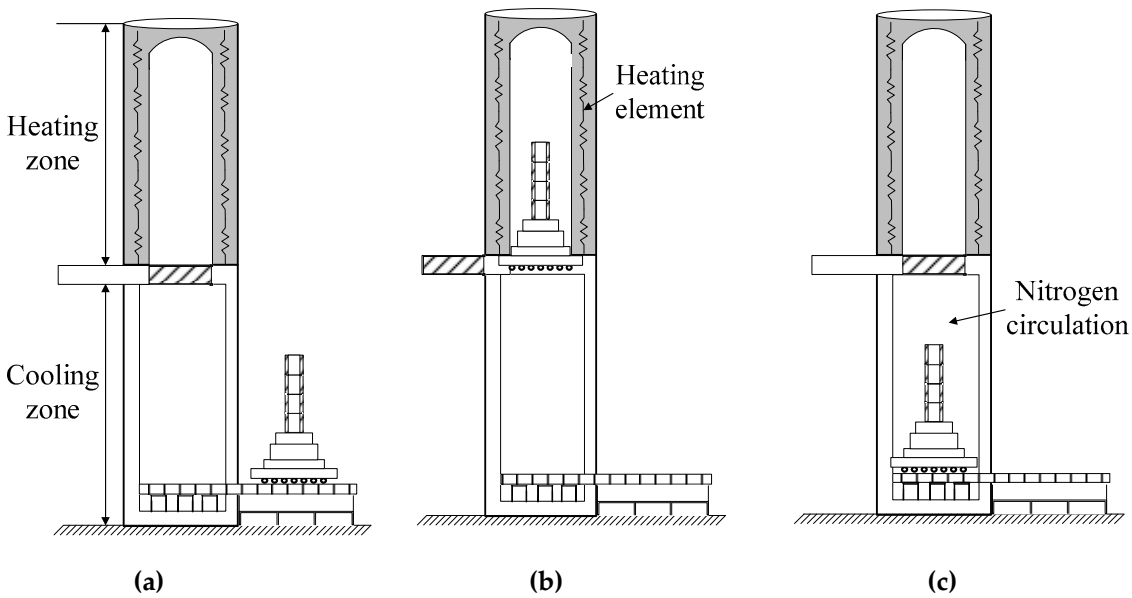

Figure 4. Schematic drawing of vertical diffusion bonding system: (**a**) Tube loading; (**b**) Heating zone—diffusion bonding; (**c**) Cooling zone—nitrogen circulation.

3. Results and Discussion

3.1. System Development to Fabricate Long Tubular Products

The diffusion bonding system developed in this study consists of an upper heating zone and a lower cooling zone. Figure 5 shows installed heating and cooling chambers on the shop floor. The total height of the system is 8.3 m, and spaces of heating and cooling chambers are 2.0 m × 2.0 m × 2.5 m, and 2.5 m × 2.0 m × 2.5 m, respectively.

(**a**) (**b**)

Figure 5. Vertical diffusion bonding system: (**a**) Upper heating zone; (**b**) Lower cooling zone.

In the heating zone, the stacked tubes are diffusion bonded by heating under a controlled atmosphere. Figure 6 provides photographs of the upper heating zone and 180 KW moly heating elements. As the moly heating element in nitrogen atmosphere can be deteriorated at high temperature, the environmental control in the heating zone is mainly required at temperatures above 760 °C.

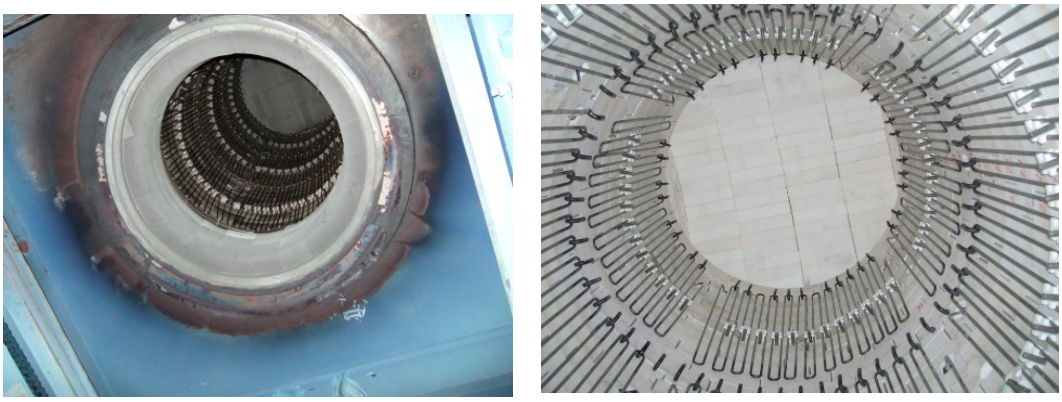

(**a**) (**b**)

Figure 6. (**a**) Upper heating zone; (**b**) Moly heating elements.

In the cooling zone, the bonded tubular products are rapidly cooled by circulating nitrogen gas. Figure 7 provides photographs of the lower cooling zone. The diffusion-bonded product is moved to the cooling zone and cooled by nitrogen circulation. The stacked tubes positioned at the heating zone are moved to the cooling zone and cooled by nitrogen circulation.

(**a**) (**b**) (**c**)

Figure 7. Workpiece movement; (**a**) workpiece in the upper heating zone; (**b**) move down to lower cooling zone; (**c**) workpiece in the lower cooling zone.

During diffusion bonding, the stacked tubes are heated and cooled under a controlled atmosphere. For the control of the workpiece movement and environmental atmosphere, the refractory valve seat, which is a movable gate valve that mates with the valve face, was used.

The unit tubes are stacked by directly putting them together "face-to-face." For tight joining, the surfaces to be joined are machined so that the outside diameter of one (protruded) is equal to the inside diameter of the other (sunken). Figure 8 shows joint preparation for best fit of contacting tubes. Unexpected power unbalances, vibrations, biased stacking, and non-uniform temperature distribution during diffusion bonding may cause distortion or buckling in stacked tubes. Figure 9 shows a sample of process-induced distortion and buckles in stacked tubes observed during preliminary tests.

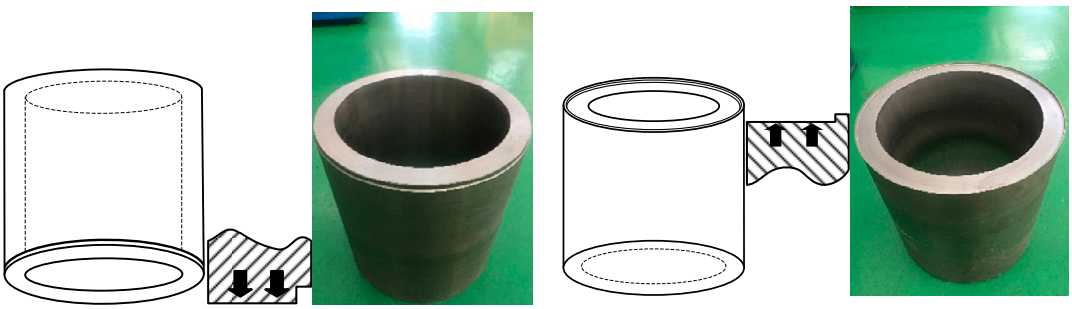

(**a**) (**b**)

Figure 8. Joint preparation for best fit: (**a**) protruded; (**b**) sunken.

Figure 9. Sample of distortion and buckles in stacked tubes.

Therefore, proper alignment or location needs to be secured with suitable support, or by applying light pressure. In this study, special supports are designed and applied to maintain the straightness and concentricity of the long tubular part. As shown in Figure 10, three round molybdenum bars are located inside of the stacked tubes, and the alignment of the bars is maintained by triangular alumina cores.

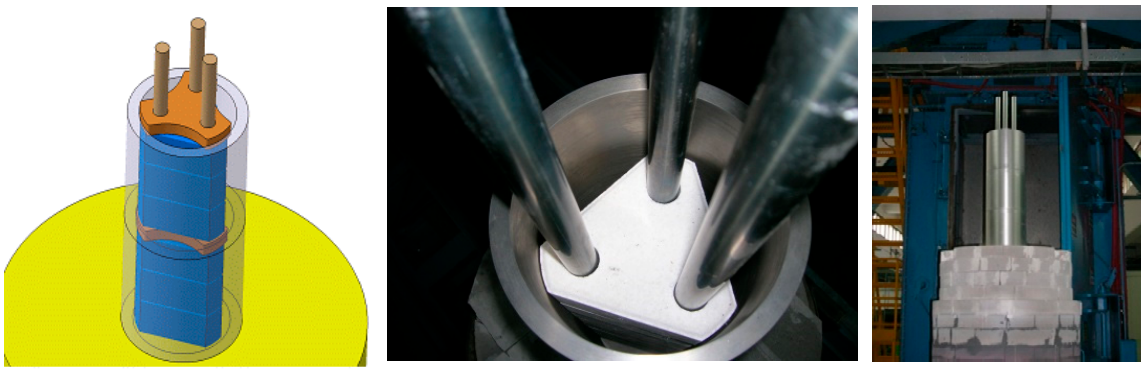

(**a**) (**b**) (**c**)

Figure 10. Supporting device to maintain straightness of stacked tubes: (**a**) conceptual view; (**b**) three round molybdenum bars are located inside of the stacked tubes; (**c**) set-up view.

3.2. Fabrication of Long Tubular Products

The estimation of the bonding performances of tubes formed by diffusion bonding processes, was made in long tubular parts by joining three-unit tubes. Diffusion bonding is subject to a time–temperature relationship. In this study, the diffusion bonding was performed under the condition of 5 h in holding time. For a given holding time, the optimal temperature to achieve the desired bonding quality was determined through the results obtained at the five different temperatures, 1427 °C, 1438 °C, 1441 °C, 1443 °C, and 1454 °C.

Two of the most important factors are the uniformity of temperature and the gas atmosphere in the heating zone. With too rapid heating to the designated temperature for diffusion bonding, the refractory brick and heating coil could be damaged. Figure 11 shows the controlled heating schedule proposed for the diffusion bonding of stacked unit tubes. If the nitrogen atmosphere is maintained at temperatures above 760 °C, the moly heating elements in the heating system become nitrided, which shortens the heating element life span. At temperatures above 760 °C, the circulating hydrogen gas in the heating zone does not deteriorate the heating system and is safely emitted and burned at the outlet.

Therefore, the constant heating rate in the heating zone is maintained until 760 °C, under a nitrogen atmosphere. Above 760 °C, the nitrogen atmosphere is substituted with a hydrogen atmosphere to activate the heating zone. During atmospheric change, the temperature of the heating zone is reduced about 30 °C, but the temperature can be stabilized with an increasing content of hydrogen gas. When the hydrogen content exceeds 99%, the temperature increases linearly to the designated temperature for diffusion bonding.

Figure 12 shows the microstructural evolution with diffusion bonding temperatures. From the microstructures shown in Figure 10, the temperature for the diffusion bonding has been determined.

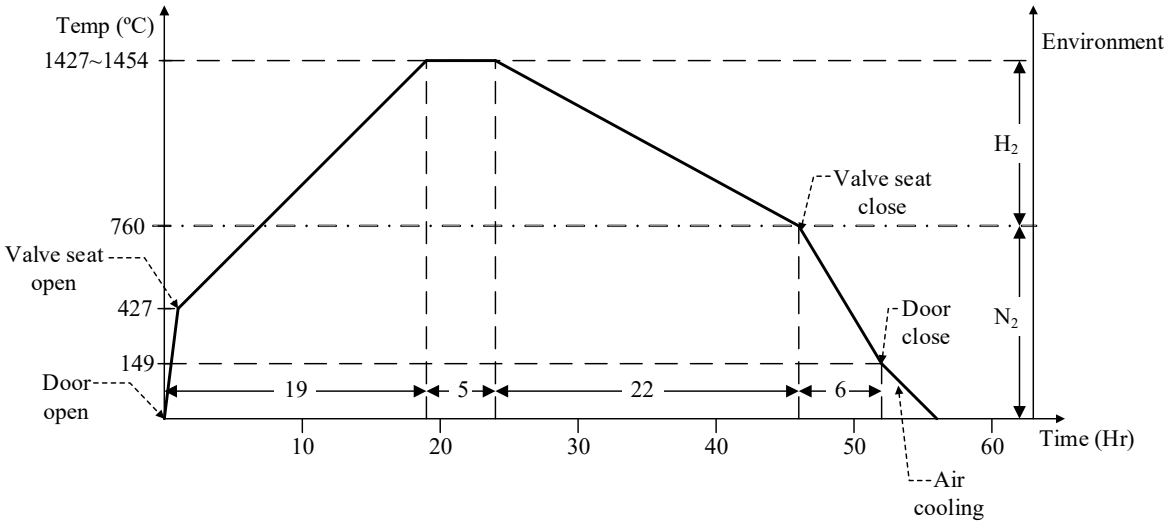

Figure 11. Processing cycle for diffusion bonding to make long tubular parts.

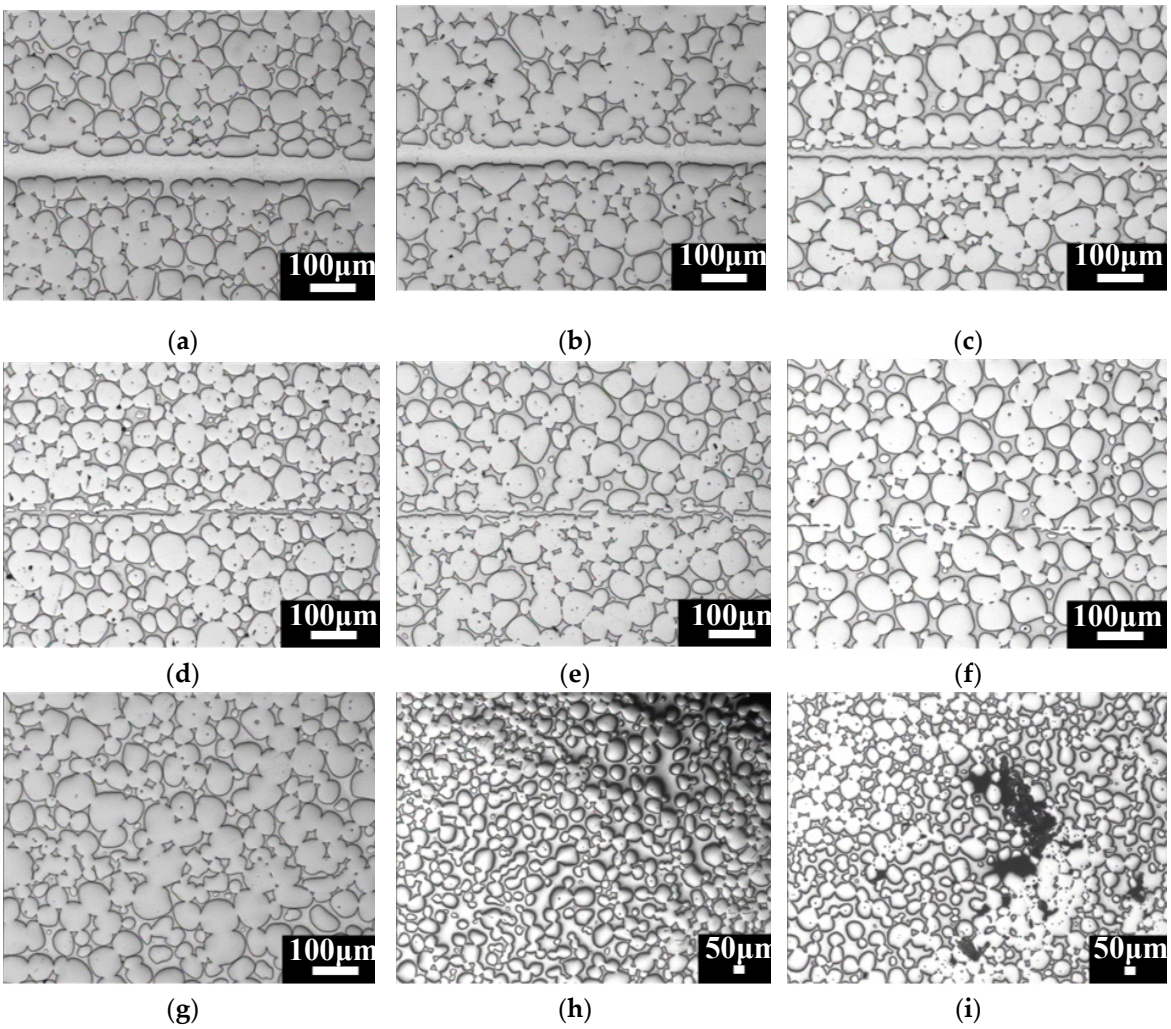

Figure 12. Microstructural evolution with diffusion bonding temperatures: (**a**) joining of binder metals starts; (**b**) width of binder layer decreases due to self-weight; (**c**) further decrease in the width of binder layer; (**d**) creation of a bonding line; (**e**) diffusion bonding of tungsten powder along with the bonding line; (**f**) bonding line disappears; (**g**) growth of tungsten powder (optimal bonding); (**h**) over-growth of tungsten; (**i**) pore generation with binder disappearance.

Table 1 shows the test result of diffusion bonding experiments obtained at various temperatures. At temperatures below the designated temperature for diffusion bonding, joining between tubes is insufficient and tubes can easily separate due to insufficient joining. At the designated temperature for diffusion bonding, joining of binder metals starts and the joining line between binders starts to decrease due to the self-weight of the tubes. Then, the movement of tungsten powder becomes active and joining lines disappear. Perfect joining can be accomplished at this stage. At temperatures above the designated temperature for diffusion bonding, tungsten powders coalesce, and irregular tungsten powders also increase. Furthermore, the binder starts to disappear and pores are generated. The microstructures obtained from the diffusion bonding test clearly show the evolution of the microstructure.

Table 1. Diffusion bonding test result.

Case	Temp (°C)	Microstructure	Bonding Quality
A	1427	Figure 12a,b,c	Bad
B	1438	Figure 12d,e	Bad
C	1441	Figure 12f	Acceptable
D	1443	Figure 12g	Good
E	1454	Figure 12h,i	Overheat (distortion)

If the designated temperature is well-maintained during diffusion bonding, the surfaces pressurized by self-weights start to join by using applied thermal energy. A sound product was obtained at 1443 °C (Case D), as shown in Figure 13a. When the applied temperature exceeds the designated temperature for diffusion bonding (Case E), the liquid phase induces dimensional distortion and degrades the bonding qualities, as shown in Figure 13b. If the temperature is lower than the designated temperature for diffusion bonding, insufficient junctures are observed. After heating for diffusion bonding, bonded tubular products are slowly cooled in the furnace to prevent thermal shock. Rapid cooling can damage the heating coils and cause failures of the refractory bricks in the heating zone. In the product extract, the hydrogen atmosphere is substituted with nitrogen atmosphere. Then, the product is moved to the cooling zone and cooled by nitrogen circulation.

Figure 14 shows a diffusion bonded tube obtained using controlled the heating schedule shown in Figure 11. The outer diameter, wall thickness, and length of the tube are 205.0 mm, 20.0 mm, and 832 mm, respectively.

In the stabilization of the material properties of the diffusion bonded tube, a post heat treatment was performed at 1150 °C for 8 h [34,35]. The bonding quality of diffusion bonded products was estimated in terms of mechanical properties such as the hardness, tensile strength, and elongation.

Table 2 shows the mechanical properties of the diffusion bonded tube after heat treatment. As shown in Table 2, no remarkable differences in mechanical properties are observed, and the bonded zone has the characteristics of the non-bonded base zone. As shown above, the proposed method was successfully implemented, and its feasibility has been well confirmed.

Table 2. Mechanical properties of the diffusion bonded tube after heat treatment.

Position	Hardness (HRC)	Tensile Properties (ASTM E8M)	
		Tensile Strength (kg/mm^2)	Elongation (%)
Bonded Zone	29.75	95.2	29.1
Non-bonded base	29.69	95.9	28.3

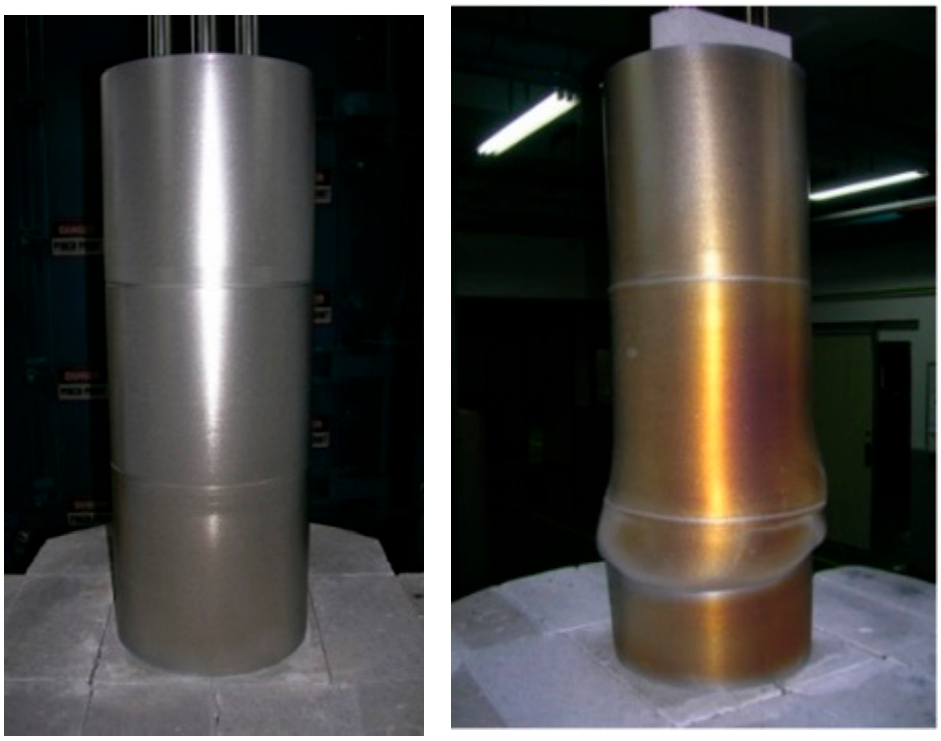

(**a**) (**b**)

Figure 13. Diffusion bonded long tubular tubes: (**a**) sound tube; (**b**) tube that has been distorted due to overheating.

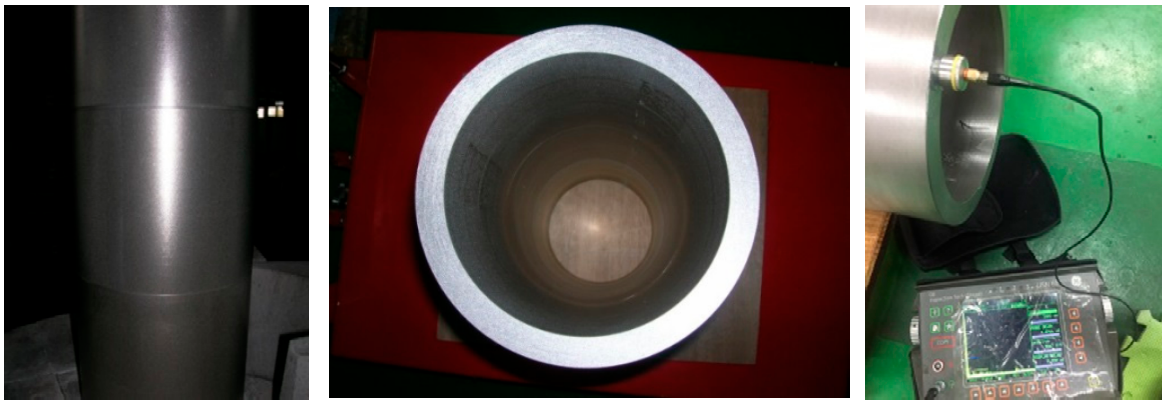

(**a**) (**b**) (**c**)

Figure 14. (**a**) Diffusion bonded tube (front view); (**b**) diffusion bonded tube (top view); (**c**) defect inspection.

4. Conclusions

A useful system to fabricate long tubular parts of THAs by diffusion bonding of two- or more-unit tubes was developed and the following conclusions were obtained:

(1) The developed system in the present study is a novel one for producing a monolithic long tubular part for a wide variety of uses. This industry-applicable tube manufacturing system was well characterized, and its feasibility was demonstrated by bond quality, which was assessed by optical metallography and mechanical testing.

(2) The diffusion bonding performance was found to be significantly influenced by the uniformity of temperature and the gas atmosphere in the heating furnace. To protect the heating furnace and to minimize distortion of products, heating and cooling rates with their respective gas atmospheres must be precisely controlled.

(3) The machining of protruded/sunken surfaces, and the three molybdenum round bars maintained by triangular alumina cores were helpful to maintain the straightness of the long tubular products.

(4) Monolithic long tubular products were successfully manufactured by diffusion bonding of the unit tubes stacked in a furnace consisting of heating and cooling zones.

(5) The microstructural evolution during diffusion bonding has been sequentially characterized at various temperatures.

Author Contributions: Data curation, S.W.H. and T.W.H.; Investigation, Z.S.P. and I.Y.O.; Software, Y.Y.W.; Validation, Y.K.; Supervision, Y.H.M. All authors have read and agreed to the published version of the manuscript.

Funding: This work was supported by the National Research Foundation of Korea (NRF) grant funded by the Korean government (MSIT) (No.2019R1A5A6099595).

Conflicts of Interest: The authors declare no conflict of interest.

References

1. Pathak, A.; Panchal, A.; Nandy, T.K.; Singh, A.K. Ternary W-Ni-Fe tungsten heavy alloys: A first principles and experimental investigations. *Int. J. Refract. Met. Hard Mater.* **2018**, *75*, 43–49. [CrossRef]
2. Panchal, A.; Nandy, T.K. Effect of composition, heat treatment and deformation on mechanical properties of tungsten heavy alloys. *Mater. Sci. Eng. A* **2018**, *733*, 374–384. [CrossRef]
3. Tehrani, M.S.; Naeini, H.M.; Hartley, P.; Khademizadeh, H. Localized edge buckling in cold roll-forming of circular tube section. *J. Mater. Process. Technol.* **2006**, *177*, 617–620. [CrossRef]
4. Moon, Y.H.; Kim, D.W.; Van Tyne, C.J. Analytical model for prediction of sidewall curl during stretch-bend sheet metal forming. *Int. J. Mech. Sci.* **2008**, *50*, 666–675. [CrossRef]
5. Yi, H.K.; Kim, D.W.; Van Tyne, C.J.; Moon, Y.H. Analytical prediction of springback based on residual differential strain during sheet metal bending. *Proc. Inst. Mech. Eng. Part C J. Mech. Eng. Sci.* **2008**, *222*, 117–129. [CrossRef]
6. Chen, W.; Jiang, J.; Li, D.; Zou, T.; Peng, Y. Flower pattern and roll positioning design for the cage roll forming process of ERW pipes. *J. Mater. Process. Technol.* **2019**, *264*, 295–312. [CrossRef]
7. Wang, F.J.; Shuang, Y.H.; Hu, J.H.; Wang, Q.H.; Sun, J.C. Explorative study of tandem skew rolling process for producing seamless steel tubes. *J. Mater. Process. Technol.* **2014**, *214*, 1597–1604. [CrossRef]
8. Kim, S.Y.; Joo, B.D.; Shin, S.; Van Tyne, C.J.; Moon, Y.H. Discrete layer hydroforming of three-layered tubes. *Int. J. Mach. Tools Manuf.* **2013**, *68*, 56–62. [CrossRef]
9. Han, S.; Woo, Y.; Hwang, T.; Oh, I.; Moon, Y.H. Tailor layered tube hydroforming for fabricating tubular parts with dissimilar thickness. *Int. J. Mach. Tools Manuf.* **2019**, *138*, 51–65. [CrossRef]
10. Yi, H.K.; Pavlina, E.J.; Van Tyne, C.J.; Moon, Y.H. Application of a combined heating system for the warm hydroforming of lightweight alloy tubes. *J. Mater. Process. Technol.* **2008**, *203*, 532–536. [CrossRef]
11. Park, J.Y.; Han, S.W.; Jeong, H.S.; Cho, J.R.; Moon, Y.H. Advanced sealing system to prevent leakage in hydroforming. *J. Mater. Process. Technol.* **2017**, *247*, 103–110. [CrossRef]
12. Rajiv, S.; Sundaram, K.S.; Narendran, C. Finite element analysis of electromagnetic compression forming of steel tubes. *Procedia Eng.* **2012**, *38*, 2520–2524. [CrossRef]
13. Park, H.; Kim, D.; Lee, J.; Kim, S.J.; Lee, Y.; Moon, Y.H. Effect of an aluminum driver sheet on the electromagnetic forming of DP780 steel sheet. *J. Mater. Process. Technol.* **2016**, *235*, 158–170. [CrossRef]
14. Nandam, S.R.; Ravikiran, U.; Rao, A.A. *Machining* of *tungsten heavy alloy* under cryogenic environment. *Procedia Mater. Sci.* **2014**, *6*, 296–303. [CrossRef]
15. Alvarado-Contreras, J.A.; Olevsky, E.A.; Maximenko, A.L.; German, R.M. A continuum approach for modeling gravitational effects on grain settling and shape distortion during liquid phase sintering of tungsten heavy alloys. *Acta Mater.* **2014**, *65*, 176–184. [CrossRef]
16. Dinçer, O.; Pehlivanoğlu, M.K.; Çalişkan, N.K.; Karakaya, İ.; Kalkanli, A. Processing and microstructural characterization of liquid phase sintered tungsten–nickel–cobalt heavy alloys. *Int. J. Refract. Met. Hard Mater.* **2015**, *50*, 106–112. [CrossRef]
17. Heaney, D.F.; German, R.M.; Ahn, I.S. The gravitational effects on low solid-volume fraction liquid-phase sintering. *J. Mech. Sci.* **1995**, *30*, 5808–5812. [CrossRef]

18. Wu, Y.; German, R.M.; Marx, B.; Bollina, R.; Bell, M. Characteristics of densification and distortion of Ni–Cu liquid-phase sintered tungsten heavy alloy. *Mater. Sci. Eng. A* **2003**, *344*, 158–167. [CrossRef]
19. Park, Z.S.; Lee, S.; Lee, T.; Kim, J.H.; Moon, Y.H. Fabrication of long tubular parts made of tungsten-heavy alloys by inductive bonding of multiple tubes. *Int. J. Refract. Met. Hard Mater.* **2019**, *85*, 105058. [CrossRef]
20. Song, M.C.; Moon, Y.H. Coupled electromagnetic and thermal analysis of induction heating for the forging of marine crankshafts. *Appl. Therm. Eng.* **2016**, *98*, 98–109. [CrossRef]
21. Kim, D.K.; Woo, Y.Y.; Park, K.S.; Sim, W.J.; Moon, Y.H. Advanced induction heating system for hot stamping. *Int. J. Adv. Manuf. Technol. Int.* **2018**, *99*, 583–593. [CrossRef]
22. Jung, H.K.; Kang, C.G.; Moon, Y.H. Induction Heating of Semisolid Billet and Control of Globular Microstructure to Prevent Coarsening Phenomena. *J. Mater. Eng. Perform.* **2000**, *9*, 12–23. [CrossRef]
23. Seo, D.M.; Hwang, T.W.; Moon, Y.H. Carbonitriding of Ti-6Al-4V alloy via laser irradiation of pure graphite powder in nitrogen environment. *Surf. Coat. Technol.* **2019**, *363*, 244–254. [CrossRef]
24. Jang, J.H.; Joo, B.D.; Van Tyne, C.J.; Moon, Y.H. Characterization of deposited layer fabricated by direct laser melting process. *Met. Mater. Int.* **2013**, *19*, 497–506. [CrossRef]
25. Li, Z.B.; Zhang, G.H.; Chou, K.C. Densification behavior of ultrafine W-Ni-Fe composite powders produced by a two-stage reduction process. *Powder Technol.* **2020**, *360*, 430–443. [CrossRef]
26. Joo, B.D.; Jang, J.H.; Lee, J.H.; Son, Y.M.; Moon, Y.H. Selective laser melting of Fe-Ni-Cr layer on AISI H13 tool steel. *Trans. Nonferrous Met. Soc. China* **2009**, *19*, 921–924. [CrossRef]
27. Park, Z.S.; Han, S.W.; Kim, J.H.; Kim, S.; Moon, Y.H. Manufacture of Tungsten Heavy Alloy Tube by Diffusion Bonding of Semicircular Tubes. *J. Mater. Eng. Perform.* **2020**, *29*, 699–711. [CrossRef]
28. Gurwell, W.E. Solid-State Sintering of Tungsten Heavy Alloys. *Mater. Manuf. Process.* **1994**, *9*, 1115–1126. [CrossRef]
29. Kim, E.S.; Lee, K.H.; Moon, Y.H. A feasibility study of the partial squeeze and vacuum die casting process. *J. Mater. Process. Technol.* **2000**, *105*, 42–48. [CrossRef]
30. Hwang, T.W.; Woo, Y.Y.; Han, S.W.; Moon, Y.H. Functionally graded properties in directed-energy-deposition titanium parts. *Opt. Laser Technol.* **2018**, *105*, 80–88. [CrossRef]
31. Jang, J.H.; Lee, J.H.; Joo, B.D.; Moon, Y.H. Flow characteristics of aluminum coated boron steel in hot press forming. *Trans. Nonferrous Met. Soc. China* **2009**, *19*, 913–916. [CrossRef]
32. Hafızoğlu, H.; Durlu, N. Effect of sintering temperature on the high strain rate-deformation of tungsten heavy alloys. *Int. J. Impact Eng.* **2018**, *121*, 44–54. [CrossRef]
33. Park, Z.S.; VanTyne, C.J.; Kim, J.; Hwang, T.W.; Kim, Y.; Moon, Y.H. Die-less manufacturing of tube by diffusion bonding of unit rods made of tungsten heavy alloy. *Int. J. Adv. Manuf. Technol.* **2020**, *106*, 1213–1221. [CrossRef]
34. Li, M.; Ruprecht, D.; Kracker, G.; Höschen, T.; Neu, R. Impact of heat treatment on tensile properties of 97W2Ni1Fe heavy alloy. *J. Nucl. Mater.* **2018**, *512*, 1–7. [CrossRef]
35. Park, Z.S.; Kim, J.; Woo, Y.Y.; Lee, H.; Kim, J.H.; Moon, Y.H. Forced circulation of nitrogen gas for accelerated and eco-friendly cooling of metallic parts. *Appl. Sci.* **2019**, *9*, 3679. [CrossRef]